European Polymer Journal 183 (2023) 111735

Contents lists available at ScienceDirect

European Polymer Journal

journal homepage: www.elsevier.com/locate/europolj

How we can improve ARGET ATRP in an aqueous system: Honey as an unusual solution for polymerization of (meth)acrylates

I. Zaborniak, P. Chmielarz [*]

Department of Physical Chemistry, Faculty of Chemistry, Rzeszow University of Technology, al. Powstańców Warszawy 6, 35-959 Rzeszów, Poland

ARTICLE INFO

Keywords:
Honey
Reducing sugars
ARGET ATRP
Aqueous environment
Miniemulsion

ABSTRACT

Aqueous solutions of various types of honey as a source of reducing sugars – glucose and fructose, were used to accelerate or control activators regeneration by electron transfer atom transfer radical polymerization (ARGET ATRP) in a homogeneous or heterogeneous environment. The aqueous or alcoholic-aqueous solution was applied for the polymerization of hydrophilic methacrylates i.e. 2-(dimethylamino)ethyl methacrylate (DMAEMA), glycidyl methacrylate (GMA), 2-hydroxyethyl methacrylate (HEMA), while the polymerization of a hydrophobic monomer – *n*-butyl acrylate (*n*BA) was conducted in miniemulsion under ion-pair and interfacial catalysis. The polymerization of DMAEMA in a honey solution accelerated the polymerization rate up to 30-fold with a significant improvement in the control over the structure of the product, namely, the polymers were characterized by narrow molecular weight distribution ($M_w/M_n = 1.33$), and initiation efficiency up to 98 %. Controlled polymerization of *n*BA was conducted in a honey-contained miniemulsion. Honey-based miniemulsion was successfully checked for the synthesis of both linear and branched polymers. The use of chemical reducing agents found in commercially available food products for polymerization is an economic concept that eliminates the need for high purity laboratory reagents, moreover, food products are widely available and therefore much cheaper. The proposed concept has great potential for industrial applications.

1. Introduction

Atom transfer radical polymerization (ATRP) is one of the few methods of synthesis of precisely-defined macromolecules with the possibility of designing both the topology and the chemical composition of polymer chains [1–5]. Over the years, many concepts of ATRP have been developed, ranging from the classical ATRP with high catalyst concentration to techniques characterized by diminished catalyst loading. Low ppm concepts are provided by continuous regeneration of metal catalyst complex, namely reduction to its active form, by application of chemical or external reducing agent [4,6]. Chemical reducing agents can play different roles in the ATRP mechanism, namely, a supplemental activator and reducing agent (SARA ATRP) [7,8], chemicals for activator regeneration by electron transfer (ARGET ATRP) [9–12], and thermal radical initiators (ICAR ATRP) [13], while external factors include electric current [14–16], ultrasonic waves [17,18], and light [19–21].

Currently, the development of ATRP techniques is aimed at improving existing concepts, both low ppm and metal-free methods, towards simple and economical solutions that have great potential for industrial applications [22]. Research directions vary from the use of other transition metals than copper (e.g. iron [23,24]) to the development of photocatalysts including non-toxic and economic substances that can replace the metal catalyst [25,26], the application of bio-based solvents [27–29], or the search for non-toxic and economical reducing agents or a reaction environment naturally containing reducing agents without the necessity to extract them [12]. Following the last above-mentioned research direction, chemical reducing agents used in ATRP are widely available in nature as vitamins [30–33], sugars [9,11,34–37], caffeine [38], and regenerate the catalyst on the basis of electron transfer in ARGET ATRP concept. The concept of application of fruit/vegetable extracts, commercially available products, or an aqueous solution of solid naturally-derived nourishments rich in reducing agents has recently appeared [12,38]. The use of food products in organic synthesis, thus replacing laboratory-grade reagents, is quite an attractive synthetic approach, mainly for economic reasons, and it simplifies reaction systems and chemical processes. This synthetic approach eliminates the necessity for using laboratory purity reagents, therefore

---

[*] Corresponding author.
E-mail address: p_chmiel@prz.edu.pl (P. Chmielarz).

https://doi.org/10.1016/j.eurpolymj.2022.111735
Received 30 October 2022; Received in revised form 23 November 2022; Accepted 26 November 2022
Available online 5 December 2022
0014-3057/© 2022 Elsevier Ltd. All rights reserved.

the proposed concept creates a cost-effective and environmentally-friendly solution. When designing modern technological processes, it is necessary to follow the principles of green chemistry. Therefore, a huge challenge in the synthesis of polymeric materials, apart from the elimination of metal catalysts, is also the replacement of organic solvents, most often with water systems [25,39–41]. The reducing agents available in nature are mainly soluble in water or are in the form of an aqueous solution, thus the mentioned concepts are fully justified in the context of both the economic and ecological aspects of the synthesis. The use of food products in technological processes raises some ethical discussions due to food insecurity for the population [42]. However, there should be a balance between the ethical aspect regarding using foodstuffs and following the principles of green chemistry, where the use of naturally-derived products, often foodstuffs or semi-finished products, limits or eliminates the use of harmful chemical reagents. Replacing laboratory-grade chemical reagents with foodstuffs also improves the quality of life due to the reduction of pollution from technological processes used to produce chemical reagents. When considering ethical aspects, it should also be noted that food products come from renewable sources.

Up to now, we demonstrated the possibility of using a lemon extract – a rich source of reducing agents i.e. ascorbic acid and citric acid, as a reaction environment for accelerating the polymerization of 2-(dimethylamino)ethyl methacrylate (DMAEMA) [12]. While the other work presents the polymerization of various methacrylates in brewed coffee solution, which is a tremendous source of caffeine – antioxidants capable of reducing the copper catalyst [38]. Inorganic sulfites applied commercially in many industrial processes as inexpensive reducing agents in food preservation – especially wine, and approved by FDA as food and beverage additives, were used as efficient reducing agents and supplemental activators for ATRP of methyl acrylate (MA) [43]. Therefore, a wide range of beverages containing inorganic sulfites can be potentially used as a polymerization environment, i.e. wine. In the present work we are focused on reducing sugars and their naturally-derived source for the reduction of metal catalysts, thus controlling the polymerization based on ATRP mechanism. Reducing sugars i.e. glucose and fructose are present in honey in high concentrations. Honey is a natural product made by bees. It is constituted mainly of monosaccharides i.e. fructose and glucose, besides water and other components in minor concentrations such as other sugars as disaccharides, proteins, enzymes, amino acids, phenolic compounds, minerals, vitamins, and organic acids. The content of reducing monosaccharides (fructose and glucose) in honey ranges from approx. 60–80 % w/w and the content of glucose and fructose are close to equal, depending on the kind of honey [44,45]. Previously laboratory purity monosaccharides were used merely a few times in ARGET ATRP as a reducing agent. Various reducing monosaccharides i.e. glucose, fructose, galactose, mannose, and sucrose, were used as an additive in conventional Cu(I)-catalyzed ATRP of *n*-butyl methacrylate (*n*BMA) in xylene to enhance polymerization rate [34]. Fructose was also applied as a reducing agent for Cu(II)-amine complexes in copper-catalyzed ATRP of styrene and methyl methacrylate (MMA) in bulk and toluene [36]. Glucose acted as a reducing agent for the polymerization of *n*-butyl acrylate (*n*BA) [35] and styrene [9] in anisole, and for copolymerization of acrylonitrile with methyl acrylate and dimethyl itaconate in dimethyl sulfoxide [46]. Recent work describes the use of glucose in the ARGET ATRP of *n*BMA from a waterlogged archaeological wood in an ethanol/water mixture [37].

In this paper, different types of honey have been used as a source of reducing sugars instead of laboratory reagents to accelerate or control ARGET ATRP in a homogeneous or heterogeneous reaction system. The aqueous or alcoholic aqueous solution was applied for the polymerization of hydrophilic methacrylates i.e. DMAEMA, glycidyl methacrylate (GMA), and 2-hydroxyethyl methacrylate (HEMA) (Scheme 1a), while the polymerization of a hydrophobic monomer –*n*BA was conducted in miniemulsion (Scheme 1b).

The use of chemical reducing agents that control polymerization, which can be found in commercially available food products, has many advantages. First of all, it is an economic concept that eliminates the need for high purity laboratory reagents, food products are widely available therefore they are much cheaper. When considering the use of honey and the monosaccharides found in it, the glucose and fructose found in honey are much cheaper reagents purchased from distributors of high purity chemicals. Namely, 1 g of glucose (96 %, used in synthesis) costs 1.44 $, while 1 g fructose costs 0.44$, which is on average around 1$. 1 g reducing sugars in honey (approx. 1.7 g of honey) costs

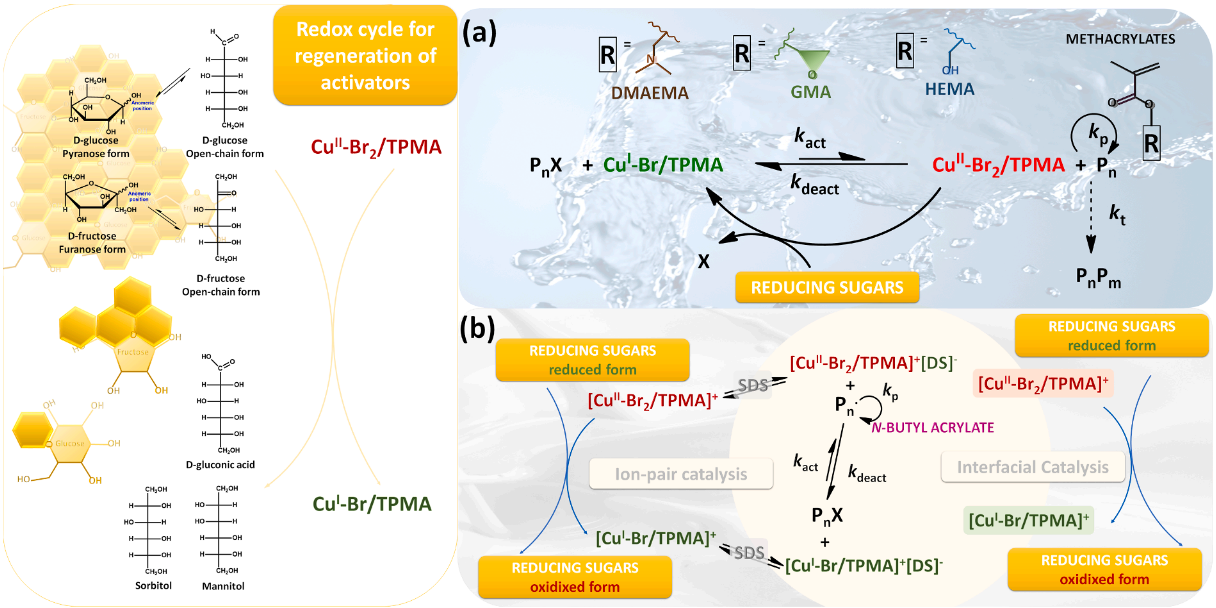

Scheme 1. Honey as a rich source of reducing agents to accelerate or control ARGET ATRP of (a) methacrylates in aqueous or alcoholic aqueous solution and (b) *n*BA in miniemulsion. Abbreviations: k_{act} – rate constant of activation, k_{deact} – rate constant of deactivation, k_p – rate constant of propagation, k_t – rate constant of termination, P_nX – initiator, $P_n^{\cdot}$ – propagating radicals, P_nP_m – terminated polymer chain; SDS – sodium dodecyl sulfate, TPMA – tris(2-pyridylmethyl)amine, X^- – halide anion.

0.017$, which is a 59-fold lower price. Considering the lack of purification of the reagents and their low cost, the concept of using food products as a source of reagents has great potential for industrial applications.

2. Results and discussion

2.1. Polymerization of DMAEMA by internally-controlled ARGET ATRP accelerated by reducing sugars present in honey

The first optimization set for the polymerization of DMAEMA in an aqueous solution included the selection of an appropriate ATRP initiator. Four molecules containing halogen atoms were studied, i.e. ethyl 2-bromoisobutyrate (EBiB), 2-hydroxyethyl 2-bromoisobutyrate (OH-EBiB), ethyl 2-bromo-phenylacetate (EBPA), and 2-bromopropionitryl (BPN, 97 %). All polymerizations were conducted in distilled water using copper(II) bromide ($Cu^{II}Br_2$) as the catalyst in the deactivated form, tris(2-pyridylmethyl) amine (TPMA) as the ligand selected on the basis of previous research [47,48], in the ratio [DMAEMA]:[Initiator]:[$Cu^{II}Br_2$/TPMA] set as 150/1/0.014. Sodium bromide (NaBr) at a concentration of 0.1 M was used as a supporting electrolyte to suppress the disassociation of the catalyst complex [12,49,50]. During the syntheses, no additional reducing agents were introduced into the reaction system, using the ability of the tertiary amine groups present in the side chains of DMAEMA to reduce the catalytic complex [12,47,48]. A summary of these reaction conditions and the characteristics of the resultant polymers is presented in Table S1. Polymerization with EBiB and OH-EBiB demonstrates comparable results i.e. slight narrowing of the molecular weight distribution (M_w/M_n, MWD) compared to other initiators (Fig. S1c,d), however, the increase in molecular weights almost stopped despite monomer conversion, reaching approximately 45 % (Fig. S1b), and consequently, the initiation efficiency was limited ($I_{eff} = 30–40$ %, Table S1, entries 1 and 2). Whereas, BPN provided the polymer product with the broadest MWD among all used ATRP initiators and slightly higher I_{eff} in relation to EBiB and OH-EBiB. As shown in entry 3 of Table S1, the use of EBPA as the initiator resulted in an MWD similar to BPN, however, the I_{eff} was significantly improved ($I_{eff} = 62$ % comparing the same time of polymerization for all syntheses). Summarizing, the results follow the previously described research for the polymerization of DMAEMA in water [48,51]. Namely, comparing the activity of the proposed ATRP initiators described by ATRP equilibrium (K_{ATRP}) the crucial aspect includes the stabilization of the radicals by substituents. Most notably, a mixed benzyl-ester initiator (i.e. EBPA) is the most active due to the synergistic stabilization effect of the phenyl and carboxyethyl groups present in its structure – phenyl and carboxyethyl. The initiator with nitrile group (BPN) is less active than EBPA, and more active than molecules with *tert*-butyl group (EBIB and OH-EBiB) [52]. The polymerization of DMAEMA in water is very fast as the monomer acts also as a reducing agent [12,47,48]. Consequently, the concentration of the reducing agent is tremendous, there is a fast generation of an active from of the copper catalyst, and therefore it is necessary to use highly active ATRP initiators. The use of a less active initiator leads to poorly controlled polymerization, which in turn leads to a lower initiation efficiency. Such an effect is visible in the case of the ATRP initiators used. The highest initiation efficiency was obtained for EBPA, therefore this molecule was used in further syntheses.

Experiments were next conducted at the optimized reaction setup with multiflorous honey solution varying honey concentration, therefore reducing sugars (RS) content and NaBr concentration (Table 1).

To precisely determine the ratio of the reducing sugars to catalyst complex in the reaction mixtures, the content of RS in multiflorous and various kinds of honey was determined by DNS assay (Fig. S2, Table S2). The synergistic effect of adjusting the appropriate concentration of RS and the concentration of an additional source of halogen has been investigated as a potential means of narrowing MWDs, with the goal of improving initiation efficiency to reduce the early termination of active chains. Namely, increasing the concentration of the reducing agent increases the copper(I) content, therefore the polymerization of DMEMA is accelerated, rate constant of activation (k_{act}) and thus K_{ATRP} are higher, which consequently leads to broader MWD [54]. To shift the ATRP equilibrium toward the inactive state to maintain adequate control over the MWD during propagation an appropriate concentration of halide salt is needed. If the concertation of halide salt is increased, the phenomenon of conversion to the alkyl halide for propagating chains occurs efficiently, therefore mitigating the rapid termination and narrowing of the MWD of the final products. Moreover, a large excess of halide salts as a source of halide anions, with respect to the catalyst prevents an excessive dissociation of halide anions from the deactivator in aqueous systems [49,50,53]. As a starting point, the 10 % w/v of honey, that is, 1,180 fold excess of reducing sugars as compared to the catalyst, and 0.1 M of halide salts were used (Table 1, entry 1). Compared to polymerization in distilled water (Table S1, entry 3), the use of honey solutions as a reaction medium significantly improved the polymerization of DMAEMA. It provided a 30-fold faster polymerization rate (compare k_p^{app}, Table S1, entry 3 vs Table 1, entry 1), reaching 98 % of DMAEMA conversion and I_{eff} equal to almost 100 % with the final product with lower dispersity ($M_w/M_n = 1.72$ vs 1.50 for polymerization in distilled water and honey solution, respectively). An introduction of an additional reducing agent to the reaction mixture besides a self-reducing monomer significantly improved the polymerization, probably due to the competitive mechanism for the reduction of copper-based catalyst by reducing sugars and DMAEMA. Therefore then the monomer had only one role in the reaction system, which prevents side reactions and allows better control of the polymerization, and provides the products

Table 1
Polymerization of DMAEMA in honey solution by ARGET ATRP.[a]

Entry	$[Honey]_0$ [% w/v]	$[NaBr]_0$[M]	t [h]	Conv[b] [%]	k_p^{app}[b]	$M_{n,theo}$[c] [$\times 10^{-3}$]	$M_{n,app}$[d] [$\times 10^{-3}$]	M_w/M_n[d]	I_{eff}[e] [%]
1	10 %	0.1	0.5	95	5.089	22,7	23,2	1.50	98
2	10 %	0.2	0.5	96	4.247	22,8	26,2	1.34	87
3	10 %	0.3	0.5	86	3.120	20,6	15,0	1.36	137
4	7.5 %	0.1	0.5	74	2.952	17,7	26,5	1.46	67
5	5 %	0.1	0.5	63	2.387	15,0	22,2	1.47	68
6	2.5 %	0.1	0.75	70	1.245	14,6	25,9	1.40	56
7	2.5 %	0.2	0.75	62	1.227	19,8	24,0	1.36	62
8	2.5 %	0.3	1.25	83	1.172	20,8	21,6	1.37	96
9	2.5 %	0.4	1.25	87	1.147	20,7	25,1	1.33	82

[a] General reaction conditions: $[DMAEMA]_0/[Initiator]_0/[Cu^{II}Br_2/TPMA]_0/[RS]_0 = 150/1/0.014/x$, x = 4, 8, 12 or 16; $V_{tot} = 10$ mL; $[DMAEMA]_0 = 3.0$ M; $[Cu^{II}Br_2/TPMA]_0 = 90$ ppm; T = room temperature (22 °C); Air atmosphere; Honey solutions in distilled water as a reaction medium.

[b] Monomer conversion and apparent rate constant of propagation (k_p^{app}) were determined by NMR [53].

[c] $M_{n,theo} = ([DMAEMA]_0/[Initiator]_0) \cdot \text{conversion} \cdot M_{DMAEMA} + M_{Initiator}$.

[d] Apparent M_n and M_w/M_n were determined by GPC.

[e] Initiation efficiency, $I_{eff} = (M_{n,theo}/M_{n,app}) \cdot 100\%$.

with lower dispersity.

By increasing the concentration of the halide salt (from 0.1 M to 0.2 M and then 0.3 M) with such an excess of the reducing agent in relation to the catalyst, the final products were obtained with a narrower M_w/M_n, while at 0.3 M NaBr (Table 1, entry 3, Fig. 1a,b) the initiation efficiency was higher than 100 %. This phenomenon indicates that the deactivation processes are too large with the additional source of halide, while the system generates a high concentration of copper (I) due to a large excess of reducing agents, which in turn leads to the formation of new propagating polymer chains.

This phenomenon was also observed when analyzing GPC traces of the polymers received using 0.2 M and 0.3 M NaBr. Namely, in the initially taken samples, bimodal signals were observed, with the content of the high molecular weight fraction decreasing along with the course of polymerization (Fig. S3b,c). Trying to decrease M_w/M_n, K_{ATRP} was decreased thus the activation equilibrium was shifted to favor the inactive polymer state slowing the overall rate of the polymerization [55]. It was performed by reducing the concentration of honey in the reaction mixture from 10 % w/v up to 2.5 % w/v (Table 1, entries 1, 4–6, Fig. 1c,d). Decreasing the RS concentration, the final products with lower dispersity were received (Fig. 1d), however, deteriorating polymerization initiation efficiency was noted (compare I_{eff}, Table 1, entries 1, 4–6). The results suggest that lower RS content decreases copper (I) concentration, thus the k_{act} was decreased providing the products with lower dispersity. However, the proposed reaction setup did not provide efficient deactivation. This led to the formation of long polymer chains with a $M_{n,app}$ overestimated in relation to the theoretical molecular weights. To improve deactivation, NaBr concentration was increased to the final value of 0.4 M (Table 1, entries 6–9, Fig. 1e,f). The use of 0.3 M (Table 1, entry 8) and 0.4 M (Table 1, entry 9) halide salt provided final polymers characterized by narrow M_w/M_n of 1.37 and 1.33, and high initiation efficiency, I_{eff} = 96 % and 82 %, respectively.

To justify the use of honey instead of reducing sugars in the form of chemical reagents, DMAEMA was polymerized in water by introducing glucose as a reducing agent in an amount equal to the content of reducing sugars in a 2.5 % w/v honey solution (Table 2).

Both RS provided polymerization characterized by linear kinetics plots (Fig. 2a) and an increase of molecular weights with monomers conversion (Fig. 2b). Despite this, honey solution enables faster polymerization rate (6-fold higher k_p^{app}) and the final polymer product with narrower M_w/M_n (Fig. 2c,d) and higher I_{eff}. Therefore, the use of RS present in honey instead of laboratory-grade glucose is fully justified. It provides more controlled polymerization and is cost-efficient, namely, 1 g of glucose (96 %, used in synthesis) costs approx. 1$, while 1 g of RS in honey (approx. 1.7 g of honey) costs 0.017$, which is a 59-fold lower price. We presume that more efficient polymerization of DMAEMA in honey instead of laboratory-grade glucose is due to the presence in the honey of other bio-elements in small concentrations (up to tens of

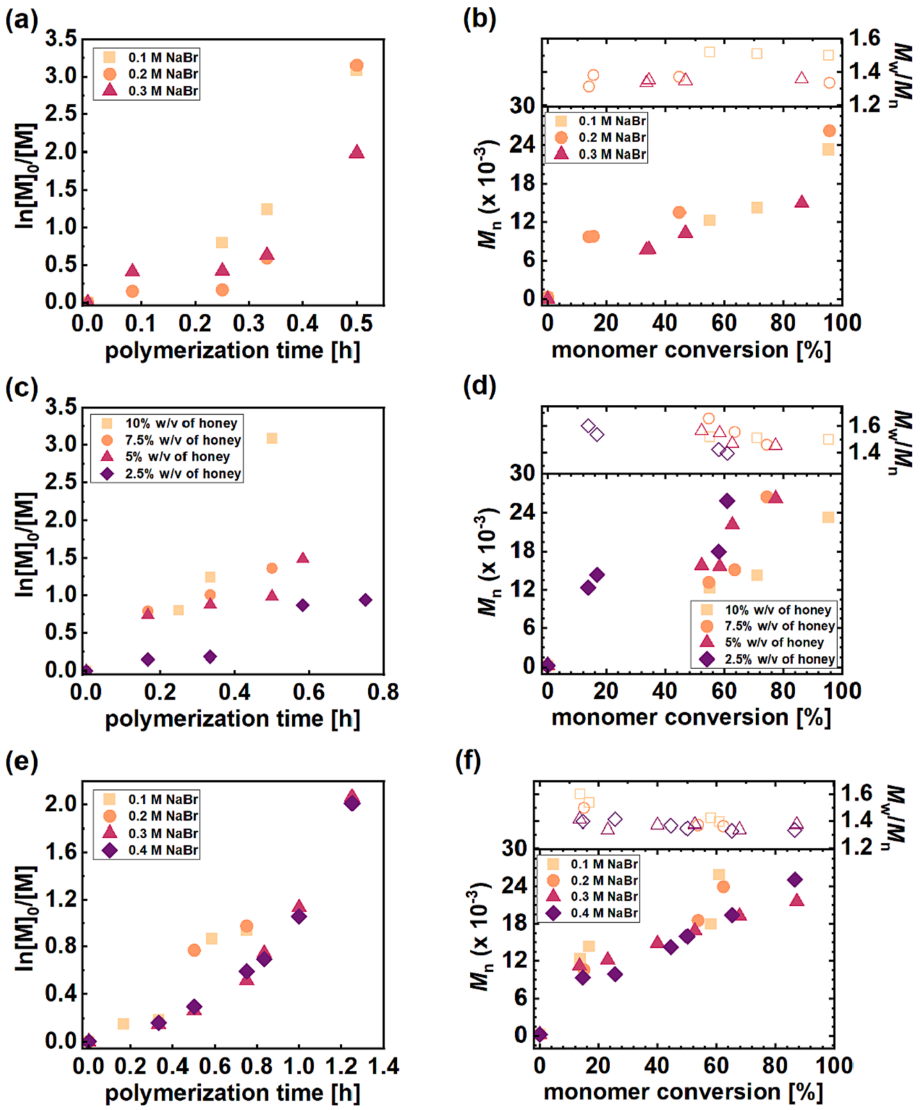

Fig. 1. Polymerization of DMAEMA by ARGET ATRP accelerated by reducing sugars present in honey. Semilogarithmic kinetic plots for polymerizations varying (a) NaBr concentration in the reaction mixture containing 10% w/v of honey, (c) honey concentration, and (e) NaBr concentration in the reaction mixture containing 2.5% w/v of honey. Evolutions of M_n and M_w/M_n vs monomer conversion for polymerizations varying (b) NaBr concentration in the reaction mixture containing 10% w/v honey, (d) honey concentration, and (f) NaBr concentration in the reaction mixture containing 2.5% w/v honey. Reactions conditions as in Table 1.

Table 2
Polymerization of DMAEMA using lab-grade glucose and reducing sugars in honey by ARGET ATRP.[a]

Entry	Source of RS	t [h]	Conv[b] [%]	k_p^{app}[b]	$M_{n,theo}$[c] [$\times 10^{-3}$]	$M_{n,app}$[d] [$\times 10^{-3}$]	M_w/M_n[d]	I_{eff}[e] [%]
1	Lab-grade glucose	3.25	49.1	0.196	11,8	17,9	1.57	66
2[f]	Honey	1.25	86.6	1.147	20,7	25,1	1.33	82

[a] General reaction conditions: $[\text{DMAEMA}]_0/[\text{Initiator}]_0/[\text{Cu}^{II}\text{Br}_2/\text{TPMA}]_0/[\text{RS}]_0 = 150/1/0.014/4$; $V_{tot} = 10$ mL; $[\text{DMAEMA}]_0 = 3.0$ M; $[\text{Cu}^{II}\text{Br}_2/\text{TPMA}]_0 = 90$ ppm; $[\text{NaBr}]_0 = 0.4$ M; T = room temperature (22 °C); Air atmosphere; Honey solutions in distilled water as a reaction medium.

[b] Monomer conversion and apparent rate constant of propagation (k_p^{app}) were determined by NMR [53].

[c] $M_{n,theo} = ([\text{DMAEMA}]_0/[\text{Initiator}]_0) \cdot \text{conversion} \cdot M_{\text{DMAEMA}} + M_{\text{Initiator}}$.

[d] Apparent M_n and M_w/M_n were determined by GPC.

[e] Initiation efficiency, $I_{eff} = (M_{n,theo}/M_{n,app}) \cdot 100\%$.

[f] Reaction results presented also in Table 1 as entry 9.

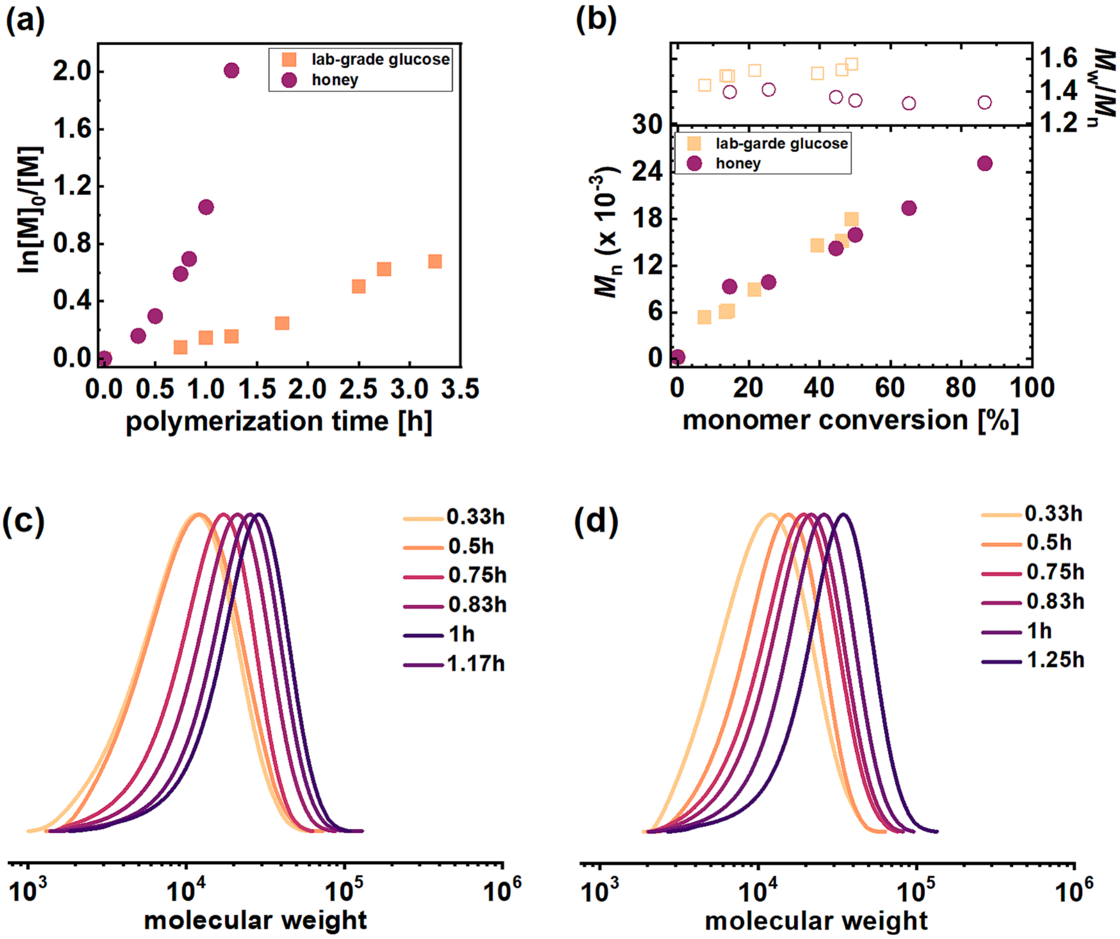

Fig. 2. Polymerization of DMAEMA by ARGET ATRP accelerated by reducing sugars present in honey and lab-grade glucose. (a) Semilogarithmic kinetic plots, (b) evolutions of M_n and M_w/M_n vs monomer conversion. GPC traces of polymers prepared using (c) lab-grade glucose and (d) reducing sugars present in honey as accelerating reducing agent. Reactions conditions as in Table 2.

thousands of ppm), namely, other carbohydrates (disaccharides, trisaccharides), low molecular mass aliphatic organic acids e.g. citric acid, gluconic acid), minerals, free amino acids, and various phenolic compounds (e.g. rutin, vanillin acid, gallic acids, caffeic acid, catechin, etc.) [44,56].

To check the effects of honey type on polymerization course, four other kinds of honey were investigated, i.e. sunflower, rapeseed honey nectar, linden, and honeydew (Table 3). All the syntheses were characterized by linear of both kinetics plots (Fig. 3a) and molecular weight increase (Fig. 3b) as a function of monomer conversion. They provided final polymers with low dispersity (M_w/M_n = 1.33 – 1.39) and high initiation efficiency – from 72 % for honeydew honey (Table 3, entry 5) to 103 % for linden honey (Table 3, entry 4).

The highest I_{eff} was provided by linden honey. Compared to other flower types of honey, it contains more B vitamins, as well as vitamin C, biotin, and niacin [57]. It is well known that vitamins can improve the control over ATRP, therefore we presume that the presence of vitamins had a positive effect on the final polymerization product. Among all kinds of honey, honeydew honey provided the final product with the broadest molecular weight distribution and lowest I_{eff}. This type of honey usually contains several times more bioelements compared to blossom kinds of honey, i.e. bioactive compounds such as phenolics, proteins, and amino acids, and also contains small amounts of vitamins A, B_2, B_6, C, PP, and K, and ash composed of minerals such as K, Ca, Na, Mg. It is the only one that contains silver, tin, molybdenum, and vanadium [44]. Despite the remarkable antimicrobial and antioxidant

Table 3
Polymerization of DMAEMA in various honey solution by ARGET ATRP.[a]

Entry	Honey type	$[RS]_0$ [% w/v]	t [h]	Conv[b] [%]	k_p^{app}[b]	$M_{n,theo}$[c] [$\times 10^{-3}$]	$M_{n,app}$[d] [$\times 10^{-3}$]	M_w/M_n[d]	I_{eff}[e] [%]
1	Multiflorous	55.8	1.25	87	1.147	20,7	25,1	1.33	82
2	Sunflower	72.7	1.25	94	1.474	22,5	27,6	1.34	81
3	Rapeseed honey nectar	66.0	1.25	89	1.003	21,2	23,7	1.35	89
4	Linden	66.4	1.17	87	1.244	20,8	20,3	1.38	103
5	Honeydew	67.3	1.0	73	1.122	17,5	24,4	1.39	72

[a] General reaction conditions: $[DMAEMA]_0/[Initiator]_0/[Cu^{II}Br_2/TPMA]_0/[RS]_0 = 150/1/0.014/4$; $V_{tot} = 10$ mL; $[DMAEMA]_0 = 3.0$ M; $[Cu^{II}Br_2/TPMA]_0 = 90$ ppm; $[NaBr]_0 = 0.4$ M; [Honey] = 2.5 % w/v; T = room temperature (22 °C); Air atmosphere; Honey solutions in distilled water as a reaction medium.

[b] Monomer conversion and apparent rate constant of propagation (k_p^{app}) were determined by NMR [53].

[c] $M_{n,theo} = ([DMAEMA]_0/[Initiator]_0) \cdot \text{conversion} \cdot M_{DMAEMA} + M_{Initiator}$.

[d] Apparent M_n and M_w/M_n were determined by GPC.

[e] Initiation efficiency, $I_{eff} = (M_{n,theo}/M_{n,app}) \cdot 100\%$; [f]Reaction results presented also in Table 1 as entry 9.

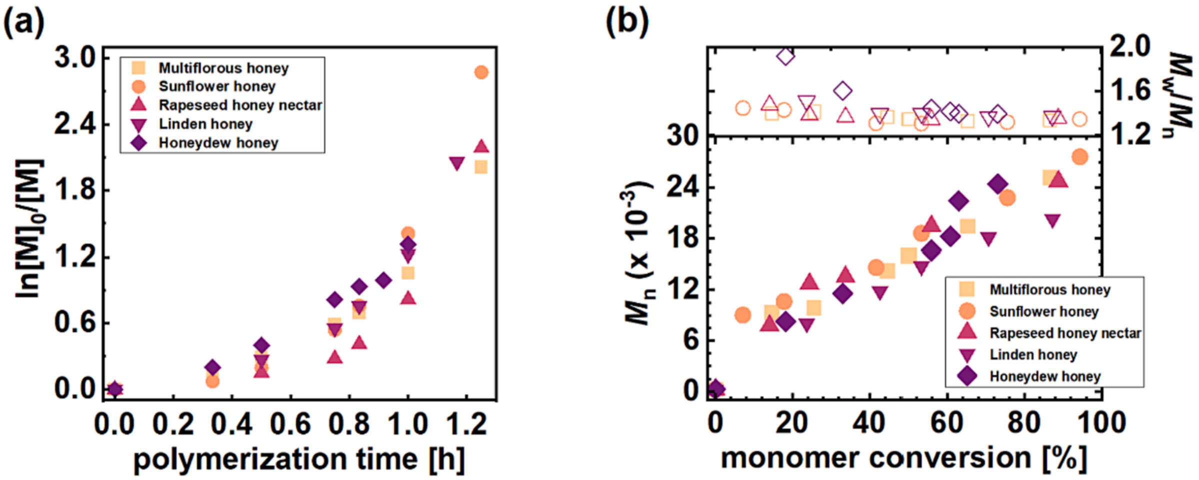

Fig. 3. Polymerization of DMAEMA by ARGET ATRP accelerated by reducing sugars present in various honey. (a) Semilogarithmic kinetic plots, and (b) evolutions of M_n and M_w/M_n vs monomer conversion. Table 3.

activity, the presence of such a high content of various bio-components in this type of honey may interfere with polymerization, therefore in this case the polymer product with the highest dispersion and the lowest I_{eff} was obtained. Considering the presence of these micro- and macroelements in honey in the context of the isolation of the final polymer product, low-molecular chemical compounds can be easily separated from the polymer using dialysis membranes with an appropriate molecular weight cutoff (MWCO). While the presence of high molecular impurities, e.g., proteins, and enzymes, requires other purification processes, such as precipitation. However, depending on the type of honey, they often contain only trace amounts of macronutrients.

2.2. Polymerization of other monomers through ARGET ATRP controlled by reducing sugars present in honey

To examine the ability of this reaction system to be extended to other polymers, the optimized conditions were then used for the polymerization of GMA, HEMA, di(ethylene glycol) methyl ether methacrylate (DEGMA), 2-hydroxyethyl acrylate (HEA) and *N*-isopropylacrylamide (NIPAM), with results summarized in Table 4 for the synthesis of PGMA and Table S3 for other polymers. The polymerizations were conducted in an inert gas atmosphere, as the monomers are not able to reduce the catalysts, therefore in the reaction setup, there is not enough reducing agent to consume additional oxygen. Synthesis of poly(glycidyl methacrylate) was carried out in an ethanol/water mixture (80/20 % v/v) due to the limited solubility in water.

The linear polymerization kinetics plots (Fig. 4a) were observed, however, there is a deviation away from a trendline of MW vs monomer conversion plot from the conversion of ca. 10 %, and the increase of the molecular weights almost ceased (Fig. 4b, Fig. S5). The negative deviation observed in MN evolution suggests a gradual accumulation of low-molecular-weight (LMW) species connected with chain activity transfer

Table 4
Polymerization of GMA in honey solution by ARGET ATRP.[a]

Entry	$[GMA]_0$ [% v/v]	$[RS]_0$ [% w/v]	t [h]	Conv[b] [%]	k_p^{app}[b]	$M_{n,theo}$[c] [$\times 10^{-3}$]	$M_{n,app}$[d] [$\times 10^{-3}$]	M_w/M_n[d]	I_{eff}[e] [%]
1	50	2.5	0.75	44	0.630	9,6	12,1	1.39	80
2	40	2.5	0.92	35	0.368	7,7	8,9	1.52	87

[a] General reaction conditions: $[GMA]_0/[Initiator]_0/[Cu^{II}Br_2/TPMA]_0/[RS]_0 = 150/1/0.015/3$ for entry 1, $[GMA]_0/[Initiator]_0/[Cu^{II}Br_2/TPMA]_0/[RS]_0 = 150/1/0.015/4$ for entry 2; $V_{tot} = 10$ mL; $[GMA]_0 = 3.7$ M for entry 1, $[GMA]_0 = 3.0$ M for entry 2; $[Cu^{II}Br_2/TPMA]_0 = 100$ ppm for entry 1 and 2; $[NaBr]_0 = 0.1$ M; T = room temperature (22 °C); Ar atmosphere; Honey in ethanol/water solution (80/20 % v/v) as a reaction medium.

[b] Monomer conversion and apparent rate constant of propagation (k_p^{app}) were determined by NMR [53].

[c] $M_{n,theo} = ([GMA]_0/[Initiator]_0) \cdot \text{conversion} \cdot M_{GMA} + M_{Initiator}$.

[d] Apparent M_n and M_w/M_n were determined by GPC.

[e] Initiation efficiency, $I_{eff} = (M_{n,theo}/M_{n,app}) \cdot 100\%$.

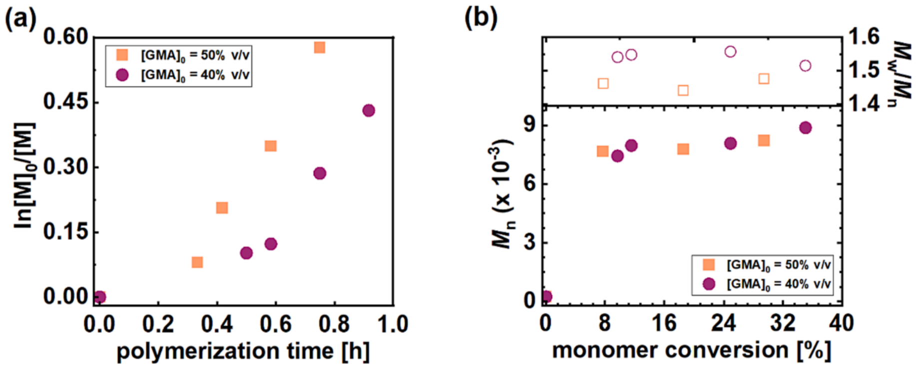

Fig. 4. Polymerization of GMA by ARGET ATRP controlled by reducing sugars present in various honey. (a) Semilogarithmic kinetic plots, and (b) evolutions of M_n and M_w/M_n vs monomer conversion. Reactions conditions as in Table 4.

on other than initiator molecules in the reaction system. In order to reduce the viscosity of the mixture as the GMA conversion progressed, and thus to obtain a higher monomer conversion, synthesis was performed with a reduced monomer concentration in the reaction system (Table 4, entry 2). The lower monomer concentration did not improve the monomer conversion and the characteristics of the final polymer product, namely, the product with higher dispersity with a slight improvement in I_{eff} was received.

Concerning the other monomers, only the polymerization of HEMA proceeded in the proposed reaction setup with honey as a source of reducing sugars (Table S3, entries 1), however, solely a few percent monomer conversion was achieved. The polymerizations of other monomers did not proceed (Table S3, entries 2–4). In previous studies, monosaccharides were used as reducing agents in ATRP only in organic solvents which are not able to form hydrogen bonds with other molecules [34–36]. In water the hydroxyl groups in monosaccharide i.e. glucose can form strong hydrogen bonds with the solvent molecules, therefore the reducing properties of monosaccharide are disrupted. In the case of DMAEMA, the monomer also serves as a reducing agent and the reducing sugars improve the polymerization [12,47,48]. Whereas GMA was reported also as an intrinsic reducing agent in ATRP in some organic solvents [58] and is capable of epoxy ring-opening reaction with polysaccharides in a protic solvent such as water [59], therefore we presume the mechanism improves the polymerization.

2.3. Polymerization of nBA through ARGET ATRP in miniemulsion controlled by reducing sugars present in honey

Further experiments were designed to extend these optimized conditions for the polymerization of a hydrophobic monomer in miniemulsion under ion-pair and interfacial catalysis. Reducing sugars present in honey were tested as reducing agents in miniemulsion ARGET ATRP of *n*BA varying targeted degree of polymerization, and a molar excess of RS to a copper catalyst (Table 5). The polymerizations were conducted in the reaction mixture composed of 18.1 % v/v *n*BA, hexadecane, and EBiB as the initiator forming the organic phase, and the anionic surfactant SDS, supporting electrolyte (NaBr), hydrophilic catalytic complex – $Cu^{II}Br_2$/TPMA dissolved in water forming continuous phase. Droplets with a hydrodynamic diameter from 94 nm to 135 nm (measured by DLS; Fig. S12) were formed before the polymerization, comparable to typical miniemulsion droplets with a diameter of approx. 100 nm [30,60,61]. While, after the polymerization, the diameter of the hydrophobic droplets somewhat increased. The most likely reason for the higher hydrodynamic diameter of the polymer particles after the polymerization is the diffusional degradation (Ostwald ripening), while small droplets disappear due to the diffusion of monomers towards the large ones. The effect of the Ostwald ripening is significantly limited by using a costabilizer, i.e. hexadecane which is a highly water-insoluble compound of low molecular weight [62].

The first experiments were designed to demonstrate the effect of the targeted degree of polymerization (DP_{target}) on the polymerization course, targeting total DP of 120, and 1,200 while using a ratio

Table 5
Polymerization of *n*BA by ARGET ATRP in honey-containing miniemulsion.[a.]

Entry	DP_{target}	$[RS]_0$ [% w/v]	$[Cu^{II}Br_2]_0/[RS]_0$	t [h]	Conv[b] [%]	k_p^{app}[b]	$M_{n,theo}$[c] [$\times 10^{-3}$]	$M_{n,app}$[d] [$\times 10^{-3}$]	M_w/M_n[d]	I_{eff}[e] [%]	$d_{Z\text{-}ave}$ [nm][f]	$d_{Z\text{-}ave}$ [nm][g]
1	1,200	10	1/379	48.8	43	0.011	71,1	74,6	1.95	95	94 ± 3	162 ± 5
2	120	10	1/379	26.25	80	0.059	12,4	12,8	2.16	97	135 ± 3	221 ± 22
3	120	0.3	1/10	22.6	91	0.098	14,1	12,8	1.54	111	112 ± 3	127 ± 2
4	120	0.05	1/2	24.7	62	0.040	9,8	10,6	2.04	92	119 ± 3	141 ± 3
5[h]	1,200	0.3	1/10	25	54	0.027 0.114[i]	95,8	42,0	1.74	228	84 ± 2	126 ± 3

[a] General reaction conditions: ARGET ATRP of *n*BA 1.7 mL (18.1 % v/v) in honey aqueous solution; $[nBA]_0/[EBiB]_0/[Cu^{II}Br_2/TPMA]_0/[RS]_0 = 1{,}200/1/0.84/318.4$ for entry 1, $[nBA]_0/[EBiB]_0/[Cu^{II}Br_2/TPMA]_0/[RS]_0 = 120/1/0.084/31.8$ for entry 2, $[nBA]_0/[EBiB]_0/[Cu^{II}Br_2/TPMA]_0/[RS]_0 = 120/1/0.084/0.8$ for entry 3, $[nBA]_0/[EBiB]_0/[Cu^{II}Br_2/TPMA]_0/[RS]_0 = 120/1/0.084/0.2$ for entry 4, $[nBA]_0/[PnBA\text{-}Br]_0/[Cu^{II}Br_2/TPMA]_0/[RS]_0 = 1{,}200/1/0.84/8.4$ for entry 5; $[HD]_0 = 10.8$ % w/w relative to *n*BA, $[NaBr]_0 = 0.1$ M, $[SDS]_0 = 6.2$ % w/w relative to *n*BA, $[Cu^{II}Br_2/TPMA]_0 = 700$ ppm; T = 65 °C; Inert gas (Ar) atmosphere.

[b] Monomer conversion and apparent rate constant of propagation (k_p^{app}) were determined by gravimetric analysis [61].

[c] $M_{n,theo} = ([nBA]_0/[Initiator]_0) \cdot conversion \cdot M_{nBA} + M_{Initiator}$.

[d] Apparent M_n and M_w/M_n were determined by GPC.

[e] Initiation efficiency, $I_{eff} = (M_{n,theo}/M_{n,app}) \cdot 100\%$.

[f] Z-Average miniemulsion droplet diameter ($d_{Z\text{-}ave}$) measured by DLS before the polymerization.

[g] Z-Average miniemulsion droplet diameter ($d_{Z\text{-}ave}$) measured by DLS after the polymerization.

[h] Chain-extention experiment, final product of the reaction from entry 3 as an ATRP initiator.

[i] k_p^{app} value determined for the polymerization time without induction period.

$[Cu^{II}Br_2]_0/[RS]_0$ equal to 1/379. Polymerization targeting DP of 1,200 (Table 5, entry 1) demonstrated the first-order kinetic plot deviated from linearity (Fig. 5a), namely, after ca. 40 h of the synthesis the monomer conversion progressed slightly, while the increase in molecular weights (Fig. 5b, Fig. S6a) was observed. This suggests decreasing in propagating radicals concentration, and the termination by coupling occurs, therefore the M_w/M_n increase. Decreasing the DP_{target} to 120 (Table 5, entry 2), deviation from the linearity on the kinetics plot was observed toward a rapid increase in the concentration of the propagating radicals (Fig. 5b). Concurrently MWs were increased to approx. 10 % of *n*BA conversion, and then almost ceased (Fig. 5b) and the bimolecular GPC traces were noticed with rapidly increased LMW fraction (Fig. S6b). The results suggest chain activity transfer, therefore new propagating chains are formed.

To yield better control during the synthesis and final products with lower dispersity, the RS concentration was decreased concerning two various excess of RS to the catalyst, 10-fold, and 2-fold. Linear first-order kinetics (Fig. 5c) and linear evolution of molecular weight with the conversion with a slight deviation of the last kinetics sample toward lower molecular weight (Fig. 5d) were observed for polymerizations in the presence of 10-fold excess of RS to the copper-based catalysts (Table 5, entry 3). The reduction of the RS concentration to 10-fold excess to the catalyst significantly decreased the dispersity of the final product (M_w/M_n = 1.54) reaching 91 % of monomer conversion. Whereas, the use of too low a concentration of reducing agent (2-fold excess to $Cu^{II}Br_2$, Table 5, entry 4) resulted in stopping the growth of molecular weights even though the conversion of the *n*BA progressed. Consequently, inefficient deactivation processes were observed, and termination by coupling of polymer chains occurred, which confirms the presence of a high molecular weight polymer fraction on GPC (Fig. S6d), and thus high dispersibility products were obtained.

To probe for the retention of alkyl bromide end groups, homopolymer chain extension was conducted for the P*n*BA with the most controlled structure (M_w/M_n = 1.54) used as a macroinitiator for the synthesis (Table 5, entry 5). Polymerization was performed while maintaining optimal conditions, such as for the synthesis of the first P*n*BA block, namely, $[nBA]_0/[PnBA\text{-}Br]_0/[Cu^{II}Br_2/TPMA]_0/[RS]_0$ = 1,200/1/0.84/8.4, increasing targeted DP to 1,200, and maintaining the same concentrations of surfactant, cosurfactant, and supporting electrolyte. The polymerization was characterized by an induction period up to approx. 18 h of the synthesis (Fig. 6a). This is associated with two possible phenomena, which are directly connected to the application of the high molecular weight initiator in the form of a polymer chain with an MW of ca. 13,000. Namely, the ATRP initiator is at a low concentration by targeting a high DP, and because of its high molecular weight, there is one initiation site in one polymer chain. Accordingly, long polymer chains can be densely packed in hydrophobic particles, and the initiation site is difficult to access, thereby disrupting the mass transport including transport of the catalyst in the form of ion pair inside the monomer drop, which can hardly reach the vicinity of the halide atom. In addition, the use of an initiator in the form of P*n*BA instead of an LMW molecule significantly increases the density of the hydrophobic droplets, which also makes the transport of the reagents difficult, thereby slowing the initiation processes. Then the linear first-order kinetics (Fig. 6a) and linear evolution of molecular weight with conversion (Fig. 6b and S6e) were observed.

Chain-extension experiment slightly broadened the M_w/M_n from the 1.54 to 1.74 for the P*n*BA macroinitiator and the final polymer product, respectively. However, the monomodal nature of the GPC signal was retained (Fig. 6c), with a low concentration of the LMW fraction, which also resulted in an inflated initiation efficiency for the final polymer sample.

2.4. Branched architecture by ARGET ATRP in miniemulsion controlled by reducing sugars present in honey

To examine the ability of this reaction system to be extended for the preparation of branched polymers, the proposed conception for the use of honey as a rich source of reducing sugars was used for the polymerization of *n*BA from macroinitiators with two – riboflavin-Br_2, and ten – troxerutin-Br_{10}, α-bromoisobutyrate initiation sites. For the synthesis of star-like polymers with troxerutin core and ten P*n*BA side chains targeted degree of polymerization and a molar excess of RS to a copper catalyst was varied (Table 6). Conversely to linear polymers, targeting a

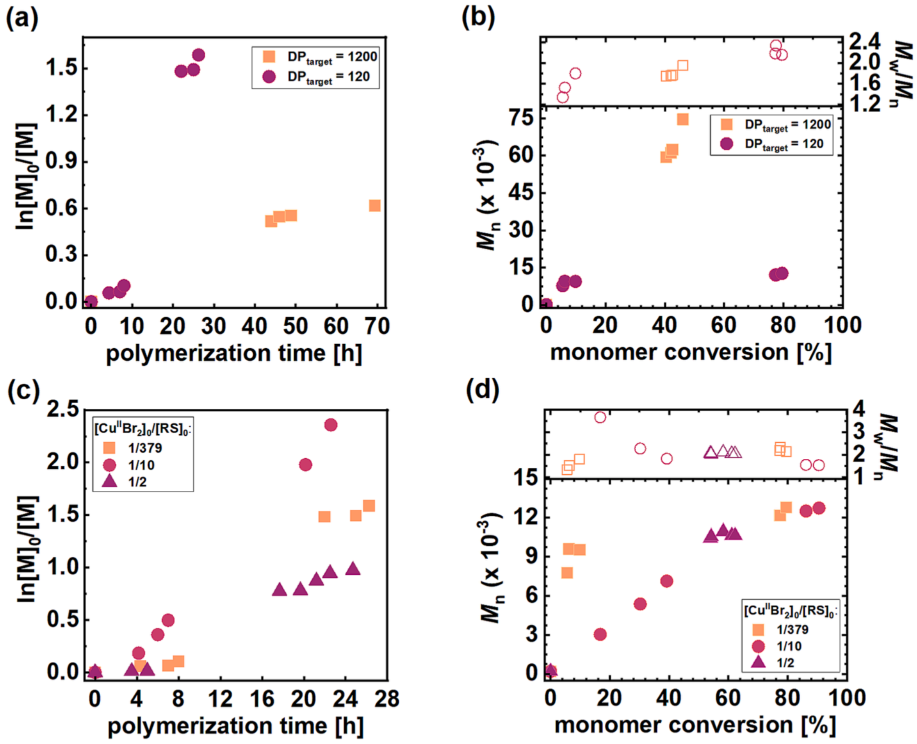

Fig. 5. The influence of targeted degree of polymerization on polymerization of *n*BA by ARGET ATRP in miniemulsion controlled by reducing sugars present honey. (a) Semilogarithmic kinetic plots, (b) evolutions of M_n and M_w/M_n vs monomer conversion. The influence of the $[Cu^{II}Br_2]_0/[RS]_0$ ratio on polymerization of *n*BA by ARGET ATRP in miniemulsion controlled by reducing sugars from honey. (c) Semilogarithmic kinetic plots, (d) evolutions of M_n and M_w/M_n vs monomer conversion. Reaction conditions as in Table 5, entry 1–4.

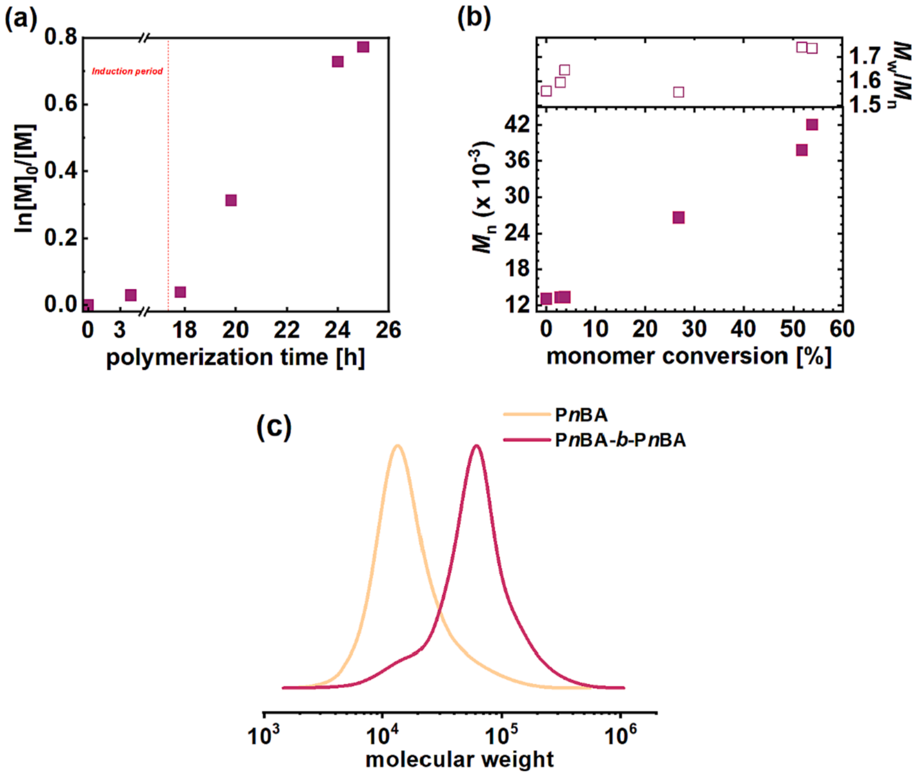

Fig. 6. Chain extension of *n*BA from P*n*BA-Br macroinitiator using honey-inspired miniemulsion ARGET ATRP controlled by reducing sugars. (a) Semilogarithmic kinetic plot, (b) evolution of M_n and M_w/M_n vs monomer conversion, (c) GPC traces. Reaction conditions are listed in Table 5, entry 5.

Table 6
Polymerization of *n*BA from Trox-Br$_{10}$ by ARGET ATRP in honey-containing miniemulsion.[a]

Entry	DP$_{target}$ (per arm)	[RS]$_0$ [% w/v]	[Cu^{II}Br$_2$]$_0$/[RS]$_0$	t [h]	Conv[b] [%]	k_p^{app}[b]	$M_{n,theo}$[c] [×10^{-3}]	$M_{n,app}$[d] [×10^{-3}]	M_w/M_n[d]	$d_{Z\text{-}ave}$ [nm][e]	$d_{Z\text{-}ave}$ [nm][f]
1	600	10	1/379	23.17	56	0.035	434,8	95,0	1.84	100 ± 1	149 ± 4
2	120	10	1/379	27.3	67	0.043	105,8	52,0	1.65	117 ± 3	170 ± 4
3	120	0.3	1/10	53.7	37	0.008	58,9	36,4	1.77	109 ± 1	125 ± 3
5[g]	1,200	10	1/379	21	41	0.025	692,6	136,4	2.05	68 ± 1	100 ± 2

[a] General reaction conditions: ARGET ATRP of 1.7 mL (18.1 % v/v) *n*BA from Trox-Br$_{10}$ in honey aqueous solution; [*n*BA]$_0$/[Trox-Br$_{10}$]$_0$/[Cu^{II}Br$_2$/TPMA]$_0$/[RS]$_0$ = 600 (per arm)/1/4.2/1,592.0 for entry 1, [*n*BA]$_0$/[Trox-Br$_{10}$]$_0$/[Cu^{II}Br$_2$/TPMA]$_0$/[RS]$_0$ = 120 (per arm)/1/0.84/318.4 for entry 2, [*n*BA]$_0$/[Trox-Br$_{10}$]$_0$/[Cu^{II}Br$_2$/TPMA]$_0$/[RS]$_0$ = 120 (per arm)/1/0.84/8.4 for entry 3, [*n*BA]$_0$/[Trox-(P*n*BA-Br)$_{10}$]$_0$/[Cu^{II}Br$_2$/TPMA]$_0$/[RS]$_0$ = 1,200 (per arm)/1/8.4/3,184.1 for entry 4; [HD]$_0$ = 10.8 % w/w relative to *n*BA, [NaBr]$_0$ = 0.1 M, [SDS]$_0$ = 6.2 % w/w relative to *n*BA, [Cu^{II}Br$_2$/TPMA]$_0$ = 700 ppm; T = 65 °C; Inert gas (Ar) atmosphere.

[b] Monomer conversion and apparent rate constant of propagation (k_p^{app}) were determined by gravimetric analysis [61].

[c] $M_{n,theo} = ([nBA]_0/[Initiator]_0) \cdot conversion \cdot M_{nBA} + M_{Initiator}$.

[d] Apparent M_n and M_w/M_n were determined by GPC.

[e] Z-Average miniemulsion droplet diameter ($d_{Z\text{-}ave}$) measured by DLS before the polymerization.

[f] Z-Average miniemulsion droplet diameter ($d_{Z\text{-}ave}$) measured by DLS after the polymerization.

[g] Chain-extention experiment, final product of the reaction from entry 2 as an ATRP initiator.

higher degree of polymerization in the reaction mixture with Trox-Br$_{10}$ did not provide more controlled polymerization. Usually, by targeting higher DP and stopping the polymerization at lower monomer conversion, the polymers with lower dispersity of the final polymer product can be achieved, because a lower dead chain fraction (DCF) is received [63]. however, for branched systems, an important issue is also the coupling of the polymer side chains, which is more likely for longer chains [64].

The polymerization targeting a degree of polymerization of 600 (Table 6, entry 1) and [Cu^{II}Br$_2$]$_0$/[RS]$_0$ ratio of 1/379 yielded polymers with two molecular weight fractions observed on GPC traces from the beginning of synthesis (Fig. S8a) suggesting coupling-coupling reactions, and the MW of the polymer almost stop to grow at conversion ca. 50 % (Fig. S7b). While decreasing of targeted DP to 120, thus conducting the synthesis of star polymers with much shorter arms provided the lower dispersity final product characterized by monomodal GPC trace (Fig. S8b). Reducing the concentration of RS significantly slower the reaction (Fig. S7c), and the value of the propagation rate constant decreased 5.4 times (compare k_p^{app}, Table 6, entries 2 and 3). There was two visible fractions on GPC traces from the beginning of the polymerization (Fig. S8c), suggesting to low concentration of propagating radicals in the reaction system, which in turn led to termination by coupling-coupling reaction and uneven growth of the star polymers. This is also proved by examining the plot of measured MW versus conversion, there is a gradual deviation away from a linear trendline at high conversion (Fig. S7d). The negative deviation observed in MW evolution suggests a gradual accumulation of low molecular weight species.

To check preserved chain end functionality of the Trox-(P*n*BA-Br)$_{10}$, the final product of the reaction described in Table 6 (entry 2) was used as a macroinitiator for chain extension experiment polymerizing the second P*n*BA block to all side chains. The polymerization proceeded with linear first-order kinetics (Fig. S9a), and progressive molecular weight evolution with conversion (Fig. S9b), however, the dispersity of the polymers increased with the increase in MW. The shift to higher molecular weight is accompanied by a clear residual peak that aligns with the original GPC trace (Fig. S9c). This suggests the presence of star-like polymers with inactive side chains in the macroinitiator, resulting in bimodal GPC traces and broadening of dispersity as polymerization proceeds. The experiment confirmed the partial retention of chain-end functionality in the first P*n*BA block.

The proposed reaction setup was also implemented for the synthesis of branched polymers with riboflavin core and two P*n*BA side arms (Table 7). Brominated riboflavin was previously examined for ARGET ATRP in miniemulsion as a triple-functional molecule [32]. It can play a role of an initiator (bromine molecules in a ribitol tail incorporated by esterification reaction), reducing agent due to the redox functionality of the isoalloxazine ring, and also enables polymerization in air conditions. In the proposed concept, RS present in honey can accelerate the polymerization as the riboflavin exhibited also reducing agent properties. The brominated riboflavin with two preserved hydroxyl groups in the ribitol tail can be placed on the surface of hydrophobic droplets, stabilizing the micelles [32]. Therefore, the first optimization set includes the polymerization of *n*BA from Rib-Br_2 under conditions selected on the basis of the synthesis of Trox-(P*n*BA-Br)$_{10}$, namely, $[n\mathrm{BA}]_0/[\mathrm{Rib\text{-}Br_2}]_0/[\mathrm{Cu^{II}Br_2/TPMA}]_0/[\mathrm{RS}]_0 = 600$ (per arm)/1/0.84/318.4, checking the possibility to remove the cosurfactant from the reaction mixture (Table 7, entries 1 and 2).

There is a large difference in the hydrodynamic diameter of the micelles formed in a dispersion system with and without a co-surfactant. For miniemulsions with hexadecane, the size of the micelles before polymerization is comparable to the standard formed systems under the given reaction conditions due to the limited Ostwald ripening effect [30,61]. After synthesis, the size of the polymer particles slightly increases (Fig. S14a). Whereas the size of the micelles in the reaction system without hexadecane is much larger, and it decreases after synthesis (Fig. S14b). This phenomenon is characteristic of emulsions in which there is a creation of new particles by secondary nucleation from the monomer in the aqueous phase. In absence of a co-stabilizer, the monomer diffusion from smaller to large particles is significant. The small particles created in that way decreased the average particle size obtained at the end of the reactions. [65]. In addition, P*n*BA polymer chains can stabilize particles, because as hydrophobic compounds, have also been used to limit the Ostwald ripening. The polymerization without HD provided first-order kinetics with negative deviation from the linearity (Fig. S10a), while the increase in the molecular weight of the polymers continued (Fig. S10b). This suggests the termination by coupling of the growing polymers, and it is proved by GPC traces, which displayed a high molecular weight shoulder (Fig. S11b). The results suggest the necessity of using a cosurfactant to form a stable miniemulsion that will ensure controlled polymerization. Analyzing the influence of targeted DP (Table 7, entry 1 vs entry 3, Fig. S10c,d) and the $[\mathrm{Cu^{II}Br_2}]_0/[\mathrm{RS}]_0$ ratio (Table 7, entry 3 vs entry 4, Fig. S10e,f) on polymerization for *n*BA from Rib-Br_2, the results follow more accurately the synthesis of homopolymers from EBiB than star-like polymers. Namely, by decreasing the $\mathrm{DP_{target}}$ from 600 to 120, the final polymer product with higher dispersity was received. While decreasing the $[\mathrm{Cu^{II}Br_2}]_0/[\mathrm{RS}]_0$ ratio from 1/379 to 1/10 initially caused the presence of two fractions on GPC traces (Fig. S11d), while the high molecular weight fraction significantly decreased as the polymerization proceeded. In consequence, the polymerization with lower RS concertation provided the final product with narrower M_w/M_n.

3. Conclusions

The paper presents an application of honey as a rich source of reducing sugars – glucose and fructose, to control ARGET ATRP in a homogenous aqueous system and heterogenous reaction environment – miniemulsion. Aqueous solutions of various types of honey were successfully used to accelerate or control ARGET ATRP in a homogeneous environment polymerizing hydrophilic methacrylates i.e. DMAEMA and GMA. The polymerization of DMAEMA in a honey aqueous solution accelerated the polymerization rate up to 30-fold with a significant improvement in the control over the structure of the final product. Namely, the final PDMAEMA products were characterized by narrow molecular weight distribution ($M_w/M_n = 1.33$), and initiation efficiency of up to 98 %. To prove the validity of using honey instead of reducing sugars in the form of laboratory reagents, the polymerization of DMAEMA in honey and with the use of pure glucose was compared. Polymerization in honey proceeded 6-fold faster and provided the product with lower dispersity and higher initiation efficiency ($M_w/M_n = 1.33$, $I_{\mathrm{eff}} = 82$ % vs $M_w/M_n = 1.57$, $I_{\mathrm{eff}} = 66$ % for honey-containing and pure glucose reaction environment, respectively). Controlled polymerization of *n*BA in a honey-contained miniemulsion system provided well-defined linear P*n*BA and branched polymers with P*n*BA side chains and a riboflavin or troxerutin core. Subsequent chain extension of the linear macromolecules and star-like polymers with *n*BA proved the livingness of the polymerization and high retention of chain-end fidelity. The use of chemical reducing agents found in commercially available food products instead of laboratory purity chemicals is an economical concept because food products are widely available therefore they are much cheaper. Comparing the price of reducing sugars in honey and high purity chemicals, the price of reducing sugars in honey is approximately 59-lower. Considering the lack of purification of the reagents and their low cost, the concept of using food products as a source of reagents has great potential for industrial applications.

Table 7
Polymerization of *n*BA from Rib-Br_2 by ARGET ATRP in honey-containing miniemulsion.[a]

Entry	$\mathrm{DP_{target}}$ (per arm)	$[\mathrm{RS}]_0$ [% w/v]	$[\mathrm{Cu^{II}Br_2}]_0/[\mathrm{RS}]_0$	t [h]	Conv[b] [%]	k_p^{app}[b]	$M_{n,theo}$[c] [$\times10^{-3}$]	$M_{n,app}$[d] [$\times10^{-3}$]	M_w/M_n[d]	$d_{Z\text{-}ave}$ [nm][e]	$d_{Z\text{-}ave}$ [nm][f]
1	600	10	1/379	4.83	67	0.211	104,1	70,1	1.64	91 ± 3	167 ± 5
2[g]	600	10	1/379	5	84	0.405	130,3	106,4	2.41	328 ± 12	206 ± 25
3	120	10	1/379	7.12	70	0.148	22,1	28,8	1.91	110 ± 1	178 ± 6
4	120	0.3	1/10	6	70	0.215	22,1	26,8	1.82	79 ± 4	95 ± 1

[a] General reaction conditions: ARGET ATRP of 1.7 mL (18.1 % v/v) *n*BA from Trox-Br_{10} in honey aqueous solution; $[n\mathrm{BA}]_0/[\mathrm{Rib\text{-}Br_2}]_0/[\mathrm{Cu^{II}Br_2/TPMA}]_0/[\mathrm{RS}]_0 = 600$ (per arm)/1/0.84/318.4 for entry 1 and 2, $[n\mathrm{BA}]_0/[\mathrm{Rib\text{-}Br_2}]_0/[\mathrm{Cu^{II}Br_2/TPMA}]_0/[\mathrm{RS}]_0 = 120$ (per arm)/1/0.17/63.7 for entry 3, $[n\mathrm{BA}]_0/[\mathrm{Rib\text{-}Br_2}]_0/[\mathrm{Cu^{II}Br_2/TPMA}]_0/[\mathrm{RS}]_0 = 120$ (per arm)/1/0.17/1.7 for entry 4, $[\mathrm{HD}]_0 = 10.8$ % w/w relative to *n*BA for entry 1, 3 and 4, $[\mathrm{HD}]_0 = 0$ % w/w relative to *n*BA for entry 2, $[\mathrm{NaBr}]_0 = 0.1$ M, $[\mathrm{SDS}]_0 = 6.2$ % w/w relative to *n*BA, $[\mathrm{Cu^{II}Br_2/TPMA}]_0 = 700$ ppm; T = 65 °C; Inert gas (Ar) atmosphere.

[b] Monomer conversion and apparent rate constant of propagation (k_p^{app}) were determined by gravimetric analysis [61].

[c] $M_{n,theo} = ([n\mathrm{BA}]_0/[\mathrm{EBiB}]_0) \cdot \mathrm{conversion} \cdot M_{n\mathrm{BA}} + M_{\mathrm{EBiB}}$.

[d] apparent M_n and M_w/M_n were determined by GPC.

[e] Initiation efficiency, $I_{\mathrm{eff}} = (M_{n,theo}/M_{n,app}) \cdot 100\%$; [e]Z-Average miniemulsion droplet diameter ($d_{Z\text{-}ave}$) measured by DLS before the polymerization.

[f] Z-Average miniemulsion droplet diameter ($d_{Z\text{-}ave}$) measured by DLS after the polymerization.

[g] Reaction mixture without HD.

CRediT authorship contribution statement

I. Zaborniak: Conceptualization, Methodology, Validation, Formal analysis, Investigation, Resources, Data curation, Visualization, Project administration, Funding acquisition, Writing - original draft, Writing - review & editing. **P. Chmielarz:** Conceptualization, Methodology, Validation, Data curation, Supervision, Project administration, Funding acquisition, Formal analysis, Writing - original draft, Writing - review & editing.

Declaration of Competing Interest

The authors declare that they have no known competing financial interests or personal relationships that could have appeared to influence the work reported in this paper.

Data availability

Data will be made available on request.

Acknowledgements

Financial support from Ministry of Science and Higher Education as a part of “Student science clubs create innovations” program (SKN/SP/534777/2022) is gratefully acknowledged. P.C acknowledges National Science Centre in Poland for the financial support as a part of the SONATA BIS 10 project (2020/38/E/ST4/00046). I.Z. acknowledges National Science Centre in Poland for the financial support as a part of the PRELUDIUM 19 project (2020/37/N/ST4/01991) and Ministry of Science and Higher Education scholarship for outstanding young scientists (SMN/16/0615/2020). NMR spectra were recorded in the Laboratory of Spectrometry, Faculty of Chemistry, Rzeszow University of Technology and were financed from budget of statutory activities.

Appendix A. Supplementary material

Experimental section, DNS assay, polymerizations results, kinetics investigation, GPC traces, DLS measurements of miniemulsion droplets, ^{1}H NMR analysis of synthesized polymers.

Supplementary data to this article can be found online at https://doi.org/10.1016/j.eurpolymj.2022.111735.

References

[1] J.O. Zoppe, N.C. Ataman, P. Mocny, J. Wang, J. Moraes, H.-A. Klok, Surface-initiated controlled radical polymerization: State-of-the-art, opportunities, and challenges in surface and interface engineering with polymer brushes, Chem. Rev. 117 (3) (2017) 1105–1318, https://doi.org/10.1021/acs.chemrev.6b00314.

[2] K. Matyjaszewski, Advanced materials by atom transfer radical polymerization, Adv. Mater. 30 (23) (2018) 1706441, https://doi.org/10.1002/adma.201706441.

[3] K. Ślusarczyk, M. Flejszar, P. Chmielarz, Less is more: A review of µL-scale of SI-ATRP in polymer brushes synthesis, Polymer 233 (2021), 124212, https://doi.org/10.1016/j.polymer.2021.124212.

[4] F. Lorandi, M. Fantin, K. Matyjaszewski, Atom transfer radical polymerization: A mechanistic perspective, J. Am. Chem. Soc. 144 (34) (2022) 15413–15430, https://doi.org/10.1021/jacs.2c05364.

[5] H. Mahdavi, M.A. Kerachian, M. Abazari, Synergistic effect of GO@SiO_2 and GO@ZnO nano-hybrid particles with PVDF-*g*-PMMA copolymer in high-flux ultrafiltration membrane for oily wastewater treatment and antifouling properties, J. Ind. Eng. Chem. 108 (2022) 374–388, https://doi.org/10.1016/j.jiec.2022.01.016.

[6] K.W. Kröckert, F. Garg, M.V. Heinz, J. Lange, P.P. Simões, R. Schmidt, O. Bienemann, A. Hoffmann, S. Herres-Pawlis, Understanding the structure–activity relationship and performance of highly active novel ATRP catalysts, Dalton Trans. 51 (35) (2022) 13272–13287, https://doi.org/10.1039/D2DT01954J.

[7] D. Konkolewicz, Y.u. Wang, P. Krys, M. Zhong, A.A. Isse, A. Gennaro, K. Matyjaszewski, SARA ATRP or SET-LRP. End of controversy? Polym. Chem. 5 (15) (2014) 4409, https://doi.org/10.1039/C4PY00149D.

[8] I. Zaborniak, A. Macior, P. Chmielarz, Smart, naturally-derived macromolecules for controlled drug release, Molecules 26 (7) (2021) 1918, https://doi.org/10.3390/molecules26071918.

[9] W. Jakubowski, K. Min, K. Matyjaszewski, Activators regenerated by electron transfer for atom transfer radical polymerization of styrene, Macromolecules 39 (1) (2006) 39–45, https://doi.org/10.1021/ma0522716.

[10] D. Yin, W. Geng, Q. Zhang, B. Zhang, Confining polymerization at emulsion interface by surface-initiated atom transfer radical polymerization on reactive Pickering stabilizer, J. Ind. Eng. Chem. 31 (2015) 360–366, https://doi.org/10.1016/j.jiec.2015.07.010.

[11] P. Karkare, S. Kumar, C.N. Murthy, ARGET-ATRP using β-CD as reducing agent for the synthesis of PMMA-*b*-PS-*b*-PMMA triblock copolymers, J. Appl. Polym. Sci. 136 (9) (2019) 47117, https://doi.org/10.1002/app.47117.

[12] I. Zaborniak, M. Sroka, P. Chmielarz, Lemonade as a rich source of antioxidants: Polymerization of 2-(dimethylamino)ethyl methacrylate in lemon extract, Polymer 254 (2022), 125099, https://doi.org/10.1016/j.polymer.2022.125099.

[13] M. Luan, D. Shen, P. Zhou, D. Li, P. Li, B. Shi, G. Wang, One-pot synthesis of block copolymer dispersant by ICAR ATRP with ppm copper catalyst and the dispersibility on pigment, Prog. Org. Coat. 169 (2022), 106914, https://doi.org/10.1016/j.porgcoat.2022.106914.

[14] P. Chmielarz, Synthesis of cationic star polymers by simplified electrochemically mediated ATRP, Express Polym. Lett. 10 (10) (2016) 810–821, https://doi.org/10.3144/expresspolymlett.2016.76.

[15] P. Chmielarz, M. Fantin, S. Park, A.A. Isse, A. Gennaro, A.J.D. Magenau, A. Sobkowiak, K. Matyjaszewski, Electrochemically mediated atom transfer radical polymerization (*e*ATRP), Prog. Polym. Sci. 69 (2017) 47–78, https://doi.org/10.1016/j.progpolymsci.2017.02.005.

[16] J. Luo, M. Chavez, C. Durante, A. Gennaro, A.A. Isse, M. Fantin, Improvement of electrochemically mediated atom transfer radical polymerization: Use of aluminum as a sacrificial anode in water, Electrochim. Acta 432 (2022), 141183, https://doi.org/10.1016/j.electacta.2022.141183.

[17] Z. Wang, F. Lorandi, M. Fantin, Z. Wang, J. Yan, Z. Wang, H. Xia, K. Matyjaszewski, Atom transfer radical polymerization enabled by sonochemically labile Cu-carbonate species, ACS Macro Lett. 8 (2) (2019) 161–165, https://doi.org/10.1021/acsmacrolett.9b00029.

[18] K. Liu, W. Zhang, L. Zong, Y. He, X. Zhang, M. Liu, G. Shi, X. Qiao, X. Pang, Dimensional optimization for ZnO-based mechano-ATRP with extraordinary activity, J. Phys. Chem. Lett. 13 (22) (2022) 4884–4890, https://doi.org/10.1021/acs.jpclett.2c01106.

[19] I. Zaborniak, P. Chmielarz, Riboflavin-mediated radical polymerization – Outlook for eco-friendly synthesis of functional materials, Eur. Polym. J. 142 (2021), 110152, https://doi.org/10.1016/j.eurpolymj.2020.110152.

[20] I. Zaborniak, A. Macior, P. Chmielarz, M. Caceres Najarro, J. Iruthayaraj, Lignin-based thermoresponsive macromolecules *via* vitamin-induced metal-free ATRP, Polymer 219 (2021), 123537, https://doi.org/10.1016/j.polymer.2021.123537.

[21] D.A. Corbin, G.M. Miyake, Photoinduced organocatalyzed atom transfer radical polymerization (O-ATRP): Precision polymer synthesis using organic photoredox catalysis, Chem. Rev. 122 (2) (2022) 1830–1874, https://doi.org/10.1021/acs.chemrev.1c00603.

[22] S. Dworakowska, F. Lorandi, A. Gorczyński, K. Matyjaszewski, Toward green atom transfer radical polymerization: Current status and future challenges, Adv. Sci. 9 (19) (2022) 2106076, https://doi.org/10.1002/advs.202106076.

[23] K. Parkatzidis, S. Boner, H.S. Wang, A. Anastasaki, Photoinduced iron-catalyzed ATRP of renewable monomers in low-toxicity solvents: A greener approach, ACS Macro Lett. 11 (7) (2022) 841–846, https://doi.org/10.1021/acsmacrolett.2c00302.

[24] Z.-H. Chen, Y. Ma, X.-Y. Wang, X.-L. Sun, J.-F. Li, B.-H. Zhu, Y. Tang, Winning strategy for iron-based ATRP using in situ generated iodine as a regulator, ACS Catalysis 10 (23) (2020) 14127–14134, https://doi.org/10.1021/acscatal.0c04312.

[25] T. Zhang, J. Yeow, C. Boyer, A cocktail of vitamins for aqueous RAFT polymerization in an open-to-air microtiter plate, Polym. Chem. 10 (34) (2019) 4643–4654, https://doi.org/10.1039/C9PY00898E.

[26] I. Zaborniak, P. Chmielarz, Comestible curcumin: From kitchen to polymer chemistry as a photocatalyst in metal-free ATRP of (meth)acrylates, J. Ind. Eng. Chem. 105 (2022) 481–490, https://doi.org/10.1016/j.jiec.2021.10.001.

[27] L. Quirós-Montes, G.A. Carriedo, J. García-Álvarez, A. Presa Soto, Deep eutectic solvents for Cu-catalysed ARGET ATRP under an air atmosphere: A sustainable and efficient route to poly(methyl methacrylate) using a recyclable Cu(II) metal–organic framework, Green Chem 21 (21) (2019) 5865–5875, https://doi.org/10.1039/C9GC02624J.

[28] A. Marathianos, E. Liarou, E. Hancox, J.L. Grace, D.W. Lester, D.M. Haddleton, Dihydrolevoglucosenone (Cyrene™) as a bio-renewable solvent for Cu(0)wire-mediated reversible deactivation radical polymerization (RDRP) without external deoxygenation, Green Chem. 22 (17) (2020) 5833–5837, https://doi.org/10.1039/D0GC02184A.

[29] V.A. Pereira, P.V. Mendonça, J.F.J. Coelho, A.C. Serra, L-menthol and thymol eutectic mixture as a bio-based solvent for the “one-pot” synthesis of well-defined amphiphilic block copolymers by ATRP, Polymer 242 (2022), 124586, https://doi.org/10.1016/j.polymer.2022.124586.

[30] Y. Wang, F. Lorandi, M. Fantin, P. Chmielarz, A.A. Isse, A. Gennaro, K. Matyjaszewski, Miniemulsion ARGET ATRP *via* interfacial and ion-pair catalysis: From ppm to ppb of residual copper, Macromolecules 50 (21) (2017) 8417–8425, https://doi.org/10.1021/acs.macromol.7b01730.

[31] E.P. Lyra, C.L. Petzhold, L.M.F. Lona, Tin(II) 2-ethylhexanoate and ascorbic acid as reducing agents in solution ARGET ATRP: A kinetic study approach by mathematical modeling and simulation, Chem. Eng. J. 364 (2019) 186–200, https://doi.org/10.1016/j.cej.2019.01.123.

[32] I. Zaborniak, K. Surmacz, M. Flejszar, P. Chmielarz, Triple-functional riboflavin-based molecule for efficient atom transfer radical polymerization in miniemulsion media, J. Appl. Polym. Sci. 137 (42) (2020) 49275, https://doi.org/10.1002/app.49275.

[33] M. Borsari, N. Braidi, M. Buffagni, F. Ghelfi, F. Parenti, N. Porcelli, G. Serafini, A. A. Isse, L. Bonifaci, G. Cavalca, A. Longo, I. Morandini, N. Pettenuzzo, Copper-catalyzed ARGET ATRP of styrene from ethyl α-haloisobutyrate in EtOAc/EtOH, using ascorbic acid/Na_2CO_3 as reducing system, Eur. Polym. J. 157 (2021), 110675, https://doi.org/10.1016/j.eurpolymj.2021.110675.

[34] A. de Vries, B. Klumperman, D. de Wet-Roos, R.D. Sanderson, The effect of reducing monosaccharides on the atom transfer radical polymerization of butyl methacrylate, Macromol. Chem. Phys. 202 (9) (2001) 1645–1648, https://doi.org/10.1002/1521-3935(20010601)202:9<1645::AID-MACP1645>3.0.CO;2-K.

[35] W. Jakubowski, K. Matyjaszewski, Activators regenerated by electron transfer for atom-transfer radical polymerization of (meth)acrylates and related block copolymers, Angew. Chem. Int. Ed. 45 (27) (2006) 4482–4486, https://doi.org/10.1002/anie.200600272.

[36] A. Dag, H. Mert, B. Dervaux, F.E. Du Prez, U. Tunca, G. Hizal, Fructose as a reducing agent for in situ generation of Cu(I) species via an electron-transfer reaction in copper-catalyzed living/controlled radical polymerization of styrene, Des. Monomers Polym. 10 (5) (2007) 425–438, https://doi.org/10.1163/156855507781833594.

[37] Y. Zhou, K. Wang, D. Hu, An aqueous approach to functionalize waterlogged archaeological wood followed by improved surface-initiated ARGET ATRP for maintaining dimensional stability, Cellulose 28 (4) (2021) 2433–2443, https://doi.org/10.1007/s10570-020-03664-y.

[38] K. Surmacz, P. Błoniarz, P. Chmielarz, Coffee beverage: A new strategy for the synthesis of polymethacrylates *via* ATRP, Molecules 27 (3) (2022) 840, https://doi.org/10.3390/molecules27030840.

[39] M. Fantin, A.A. Isse, K. Matyjaszewski, A. Gennaro, ATRP in water: Kinetic analysis of active and super-active catalysts for enhanced polymerization control, Macromolecules 50 (7) (2017) 2696–2705, https://doi.org/10.1021/acs.macromol.7b00246.

[40] I. Zaborniak, P. Chmielarz, K. Matyjaszewski, Synthesis of riboflavin-based macromolecules through low ppm ATRP in aqueous media, Macromol. Chem. Phys. 221 (4) (2020) 1900496, https://doi.org/10.1002/macp.201900496.

[41] M. Flejszar, P. Chmielarz, J. Smenda, K. Wolski, Following principles of green chemistry: Low ppm photo-ATRP of DMAEMA in water/ethanol mixture, Polymer 228 (2021), 123905, https://doi.org/10.1016/j.polymer.2021.123905.

[42] T. Gomiero, M.G. Paoletti, D. Pimentel, Biofuels: Efficiency, ethics, and limits to human appropriation of ecosystem services, J. Agric. Environ. Ethics 23 (5) (2010) 403–434, https://doi.org/10.1007/s10806-009-9218-x.

[43] C.M.R. Abreu, P.V. Mendonça, A.C. Serra, A.V. Popov, K. Matyjaszewski, T. Guliashvili, J.F.J. Coelho, Inorganic sulfites: Efficient reducing agents and supplemental activators for atom transfer radical polymerization, ACS Macro Lett. 1 (11) (2012) 1308–1311, https://doi.org/10.1021/mz300458x.

[44] S.K.T. Seraglio, B. Silva, G. Bergamo, P. Brugnerotto, L.V. Gonzaga, R. Fett, A.C. O. Costa, An overview of physicochemical characteristics and health-promoting properties of honeydew honey, Food Res. Int. 119 (2019) 44–66, https://doi.org/10.1016/j.foodres.2019.01.028.

[45] B. Pacholczyk-Sienicka, G. Ciepielowski, J. Modranka, T. Bartosik, Ł. Albrecht, Classification of polish natural bee honeys based on their chemical composition, Molecules 27 (15) (2022) 4844, https://doi.org/10.3390/molecules27154844.

[46] I.D. Grishin, S.A. Stakhi, D.Y. Kurochkina, D.F. Grishin, Controlled copolymerization of acrylonitrile with methyl acrylate and dimethyl itaconate *via* ARGET ATRP mechanism, J. Polym. Res. 25 (12) (2018) 261, https://doi.org/10.1007/s10965-018-1653-9.

[47] H. Dong, K. Matyjaszewski, ARGET ATRP of 2-(dimethylamino)ethyl methacrylate as an intrinsic reducing agent, Macromolecules 41 (19) (2008) 6868–6870, https://doi.org/10.1021/ma8017553.

[48] C.N. Britten, K. Lason, K.B. Walters, Facile synthesis of tertiary amine pendant polymers by Cu^0-mediated ATRP under aqueous conditions, Macromolecules 54 (22) (2021) 10360–10369, https://doi.org/10.1021/acs.macromol.1c01234.

[49] P. Chmielarz, S. Park, A. Simakova, K. Matyjaszewski, Electrochemically mediated ATRP of acrylamides in water, Polymer 60 (2015) 302–307, https://doi.org/10.1016/j.polymer.2015.01.051.

[50] A. Michieletto, F. Lorandi, F. De Bon, A.A. Isse, A. Gennaro, Biocompatible polymers *via* aqueous electrochemically mediated atom transfer radical polymerization, J. Polym. Sci. 58 (1) (2020) 114–123, https://doi.org/10.1002/pola.29462.

[51] F. Zeng, Y. Shen, S. Zhu, R. Pelton, Atom transfer radical polymerization of 2-(dimethylamino)ethyl methacrylate in aqueous media, J. Polym. Sci., Part A-1: Polym. Chem. 38(20) (2000) 3821-3827. https://doi.org/10.1002/1099-0518(20001015)38:20<3821::AID-POLA130>3.0.CO;2-G.

[52] W. Tang, Y. Kwak, W. Braunecker, N.V. Tsarevsky, M.L. Coote, K. Matyjaszewski, Understanding atom transfer radical polymerization: Effect of ligand and initiator structures on the equilibrium constants, J. Am. Chem. Soc. 130 (32) (2008) 10702–10713, https://doi.org/10.1021/ja802290a.

[53] V.A. Williams, T.G. Ribelli, P. Chmielarz, S. Park, K. Matyjaszewski, A silver bullet: Elemental silver as an efficient reducing agent for atom transfer radical polymerization of acrylates, J. Am. Chem. Soc. 137 (4) (2015) 1428–1431, https://doi.org/10.1021/ja512519j.

[54] G.R. Jones, Z. Li, A. Anastasaki, D.J. Lloyd, P. Wilson, Q. Zhang, D.M. Haddleton, Rapid synthesis of well-defined polyacrylamide by aqueous Cu(0)-mediated reversible-deactivation radical polymerization, Macromolecules 49 (2) (2016) 483–489, https://doi.org/10.1021/acs.macromol.5b01994.

[55] E. Mastan, S. Zhu, A molecular weight distribution polydispersity equation for the ATRP system: Quantifying the effect of radical termination, Macromolecules 48 (18) (2015) 6440–6449, https://doi.org/10.1021/acs.macromol.5b01525.

[56] M.T. Iglesias, C. de Lorenzo, M.D.C. Polo, P.J. Martín-Álvarez, E. Pueyo, Usefulness of amino acid composition to discriminate between honeydew and floral honeys. Application to honeys from a small geographic area, J. Agric. Food Chem. 52 (1) (2004) 84–89, https://doi.org/10.1021/jf030454q.

[57] M. Ciulu, S. Solinas, I. Floris, A. Panzanelli, M.I. Pilo, P.C. Piu, N. Spano, G. Sanna, RP-HPLC determination of water-soluble vitamins in honey, Talanta 83 (3) (2011) 924–929, https://doi.org/10.1016/j.talanta.2010.10.059.

[58] S.R. Woodruff, B.J. Davis, N.V. Tsarevsky, Epoxides as reducing agents for low-catalyst-concentration atom transfer radical polymerization, Macromol. Rapid Commun. 35 (2) (2014) 186–192, https://doi.org/10.1002/marc.201300696.

[59] A.V. Reis, M.R. Guilherme, T.A. Moia, L.H.C. Mattoso, E.C. Muniz, E.B. Tambourgi, Synthesis and characterization of a starch-modified hydrogel as potential carrier for drug delivery system, J. Polym. Sci. Polym. Chem. 46 (7) (2008) 2567–2574, https://doi.org/10.1002/pola.22588.

[60] M. Fantin, P. Chmielarz, Y. Wang, F. Lorandi, A.A. Isse, A. Gennaro, K. Matyjaszewski, Harnessing the interaction between surfactant and hydrophilic catalyst to control *e*ATRP in miniemulsion, Macromolecules 50 (9) (2017) 3726–3732, https://doi.org/10.1021/acs.macromol.7b00530.

[61] R. Yin, P. Chmielarz, I. Zaborniak, Y. Zhao, G. Szczepaniak, Z. Wang, T. Liu, Y. Wang, M. Sun, H. Wu, J. Tarnsangpradit, M.R. Bockstaller, K. Matyjaszewski, Miniemulsion SI-ATRP by interfacial and ion-pair catalysis for the synthesis of nanoparticle brushes, Macromolecules 55 (15) (2022) 6332–6340, https://doi.org/10.1021/acs.macromol.2c01114.

[62] J.M. Asua, Miniemulsion polymerization, Prog. Polym. Sci. 27 (7) (2002) 1283–1346, https://doi.org/10.1016/S0079-6700(02)00010-2.

[63] P. Krys, K. Matyjaszewski, Kinetics of atom transfer radical polymerization, Eur. Polym. J. 89 (2017) 482–523, https://doi.org/10.1016/j.eurpolymj.2017.02.034.

[64] I. Zaborniak, P. Chmielarz, M.R. Martinez, K. Wolski, Z. Wang, K. Matyjaszewski, Synthesis of high molecular weight poly(*n*-butyl acrylate) macromolecules *via* *se*ATRP: From polymer stars to molecular bottlebrushes, Eur. Polym. J. 126 (2020), 109566, https://doi.org/10.1016/j.eurpolymj.2020.109566.

[65] L.L. Hecht, C. Wagner, K. Landfester, H.P. Schuchmann, Surfactant concentration regime in miniemulsion polymerization for the formation of MMA nanodroplets by high-pressure homogenization, Langmuir 27 (6) (2011) 2279–2285, https://doi.org/10.1021/la104480s.